Research Article

Ferrofluid-based on Cobalt ferrite (CoFe₂O₄) Nanoparticles as Green Materials for Detection Trace-level of Uric Acid in The Human Urine Sample

Hossein Dadras Moghaddam[ORCID], Rouhollah Khani*

Department of Chemistry, Faculty of Science, University of Birjand, Birjand 97179-414, Iran

PAPER INFO	ABSTRACT
	This study was conducted to develop liquid-phase microextraction approach using ferrofluid based on cobalt ferrite nanoparticles coupled with UV–Vis spectrophotometry (LPME-FF-UV-Vis) as a simple, green, inexpensive, available and high efficiency method for separation/pre-concentration and determination trace-level of uric acid (UA) in biological samples. First, CoFe₂O₄ nanoparticles were synthesized by hydrothermal method and characterized by Fourier transform infrared (FT-IR) spectroscopy, X-ray diffraction (XRD), vibrating sample magnetometer (VSM), energy dispersive X-ray spectroscopy (EDXS), field emission scanning electron microscopy (FE-SEM), and thermogravimetric analysis (TGA). Based on preliminary studies and experiments, four parameters including pH, ferrofluid volume, temperature and ultrasonic time were selected as influential variables and optimized by central composite design (CCD). Under optimal conditions the calibration curve was linear in the concentration range of 0.42–238 μM and the limit of detection was obtained 0.12 μM. Also, the relative standard deviation for the repeatability and reproducibility were 2.1% and 3.0 %, respectively. Finally, the efficiency of LPME-FF-UV-Vis method was investigated for the detection and trace quantification of UA in human urine samples and validated via the analysis of the selected real samples by the high performance liquid chromatography-ultraviolet detection (HPLC-UV) as a reference method. The relative recovery percentages above 94 % for determination of UA confirmed the accuracy and efficiency of the proposed method.

---

*.**corresponding author:** Associate Professor of Analytical Chemistry *.E-mail address: rouhollah.khani@birjand.ac.ir*

1. Introduction

Uric acid (UA) is a biologically active compound and a final product of purine metabolism, the most crucial nitrogenous compound in urine. UA, which is produced in the human body from purines derived from food consumption or endogenous synthesis, finally excreted from the body with urine or feces. The most critical biological sources of UA are blood and urine. It is also found in food sources such as liver and beef and mutton, sausages and fatty foods [1-3]. About 70% of UA is excreted daily through urine and the rest is returned to the blood. Because UA is derived from the breakdown of purine, the concentration of UA is dependent on purine metabolism and is within a reasonable range for a healthy human [4]. At a certain pH, UA ionizes and mainly forms urate ions. When the urate concentration in the body exceeds the solubility level, sodium urate crystallizes in soft tissues and joints, leading to severe diseases such as hyperuricemia, hypertension, gout, kidney disorder, and arthritis [5, 6]. In addition, recently, due to the epidemic of coronavirus disease 2019 (COVID-19), which is caused by the acute respiratory syndrome coronavirus 2 (SARS-CoV-2), favipiravir is widely used as an antiviral agent. However the most common side effect of favipiravir is increased blood UA levels [7]. On the other hand, abnormally low UA levels can cause other diseases, such as multiple sclerosis [4]. So, the determination and quantification of UA in biological samples is extremely needed for the prevention, diagnosis and treatment of related diseases.

So far, various analytical approaches such as spectrophotometry [8], spectrofluorimetry [9], electrochemically [10], chemiluminescence [11], colorimetric [12], and high-performance liquid chromatography (HPLC) [13] have been employed for the detection of UA. Among these methods, spectrophotometry is preferred for the detection of

UA due to its low cost, acceptable sensitivity, and availability, as well as repeatability and simplicity. To reduce or eliminate the interfering effects of the sample matrix and to obtain a measurable amount of desired analyte, a sample preparation process is required before instrumental analysis [14, 15]. Analytical chemists are paying very much attention in developing selective and sensitive separation/preconcentration method for the determination of targeted trace level analytes from complex sample matrix. These methods are based on scheming easy, cheap and simple sample preparation procedures. Solid phase-extraction and liquid-liquid extraction methods are known as the most common separation/preconcentration procedures in extraction studies [16-18]. According to Green Chemistry principles, the most of extraction methods are very time and reagent consumption. A clear trend in sample preparation is miniaturization of the volume of organic solvent and extraction time. Liquid-phase microextraction (LPME), as an alternative to traditional preparation methods, has been increasingly applied to extract trace level target compounds in complex samples and used to overcome many of the disadvantages of traditional methods [19]. New approaches regarding sample preparation include the use of miniaturized and "green" methods with to realize the principles of green chemistry [20]. Recently, instead of using toxic and hazardous solvents, alternative solvents such as deep eutectic solvents (DES) [21], ionic liquids (ILs) [22], ferrofluids (FFs) [23], and supramolecular solvents (Ss) [24] are used in analytical extractions to realize green chemistry approaches.

Ferrofluids (FFs) are a group of magnetically controllable fluids have been widely used recently in processes that require both fluidity and magnetic properties of materials [25]. FF is a stable colloidal system consisting of magnetic nanoparticles

(MNPs) suspended in a liquid, which is often an organic solvent, and is called a carrier liquid. The two unique features of FFs, fluidity, and magnetism, have introduced them as suitable adsorbents that can be used as an alternative to toxic and hazardous organic solvents in extraction methods. γ-Fe_2O_3, Fe_3O_4, $NiFe_2O_4$ and $CoFe_2O_4$ are common MNPs used in the structure of ferrofluids [26]. Among these nanoparticles, cobalt ferrite or $CoFe_2O_4$, with an inverse spinel structure, has high saturation magnetism and unique chemical and mechanical stability, ease of recovery and regeneration, considerable specific surface area, which results in higher adsorption capacity and is a suitable option to be used as a nanoparticle in the preparation of ferrofluids [27]. The main advantage of FFs is that the carrier liquid can be moved using a magnetic field. So, FFs can be placed at the target location. A new class of solvents that have replaced the organic solvents of the LPME method are supramolecular solvents (Ss) that can be used as carrier liquids in the structure of ferrofluids [28]. These solvents have two essential features, one is the ability to establish various interactions with different analytes, such as hydrogen bonding, ionic and hydrophobic interaction, and secondly, Ss have a rich amphiphilic structure, which makes many active sites available for analyte extraction [29]. FFs can be rapidly injected into the sample solution and dispersed throughout it. As a result, a large surface of them is in contact with the target analytes, which accelerates the mass transfer and significantly reduces the extraction time. Also, in separation methods, FFs eliminate the use of remarkable and complicated instrumentals before the final detection [30, 31]. Generally, the convenient separation and retrieval of the extracting solvent after extraction is of crucial importance in the microextraction methods. Most of these methods require different processing steps, such as centrifugation, refrigeration to freeze the

extracting solvent, manually retrieving it to let it thaw, and the use of special equipment and additional materials [32-34]. Recently, ferrofluids as a unique magnetic colloidal system because of their significant advantages including simplicity of operation, rapidity and minimum requirements for organic solvents, and most importantly, high magnetic properties and fast fluidity have been suggested as the extracting solvent to overcome these drawbacks [35]. Accordingly, a new ferrofluid-based liquid-liquid microextraction method consisting of $CoFe_2O_4$ nanoparticles coupled with UV–Vis spectrophotometry (LLME-FFs-UV-Vis) was used to extract and determine UA from human urine samples. In this work, influential parameters of pH, ferrofluid volume, temperature, and ultrasonic time were inspected and optimized by central composite design (CCD). Then, the relevant analytical parameters were inspected. Finally, the obtained results are compared with the results of other reported methods. The proposed LLME-FF technique can be effectively enhancing the extraction efficiency, offering rapid separation, and save operation time.

2. Experimental

2.1. Reagents, solutions, apparatus and software

Uric acid was purchased from Merck Company of Germany and HCl and sodium acetate and acetic acid were obtained from sigma Aldrich Company of USA. Acetate buffer (pH=5, 1M) was used for pH adjustment. Standard solution of uric acid was prepared at a concentration 5.95 μM in distilled water. Also, the working standard solutions were prepared by appropriate dilution of standard solutions with distilled water to the desired concentration. The fourier transform infrared spectrum (FT-IR) of the $CoFe_2O_4$ magnetic nanoparticles was prepared using a spectroscopy device model 370 AVATAR manufactured by the American company Nicolt. Spectrophotometer UV–

Vis 2501 PC of the Japanese company Shimadzu was applied for recording UV–Vis spectra. The pH meter model 2211 HI of the American company HANNA was used to adjust the pH of the solutions. Experimental Design software (DOE) version 10.0 (Minneapolis, MN, USA) was used to optimize the factors affecting the extraction process.

2.2. Synthesis of ferrofluid based on CoFe₂O₄ nanoparticles

$CoFe_2O_4$ magnetic nanoparticles were synthesized by hydrothermal method. First, equal volumes of Fe $(NO_3)_3 \cdot 9H_2O$, $CoCl_2 \cdot 6H_2O$, and CTAB (with concentrations of 0.85 M, 0.425 M, and 0.85 M, respectively) were added together and mixed until a homogeneous mixture was formed. After that, while the solution was stirred by a magnetic stirrer, concentrated NaOH solution was added until the pH reached 13.0. The mixture was then transferred to a stainless steel autoclave and placed in an oven at 120°C for three hours. Eventually, black precipitates were obtained. These sediments were washed several times with distilled water and finally with ethanol to remove impurities. After the sediment was dried overnight at 70°C in the oven, $CoFe_2O_4$ nanoparticles were ground and used [36].

In order to prepare supramolecular solvent (Ss), three types of solvents (1-octanol, 1-decanol, and decanoic acid) with THF (dispersion solvent) were examined. 1-Decanol-THF resulted in the highest response (%ER UA) compared to other supramolecular solvents due to the increased micellar aggregation and was used as Ss in the subsequent experiments.

25.0 mg of synthesized $CoFe_2O_4$ nanoparticles were mixed with 5.0 mL of supramolecular solvent (1-Decanol-THF) in a 5.0-mL volumetric flask for 15 min using an ultrasonic bath at room temperature. Then, the insoluble matter was removed with an external magnet. Finally, a low-density dark brown magnetic fluid was obtained. The resulting ferrofluid was stable for three weeks.

2.3. LPME-FF procedure and preparation of real sample

A certain amount of UA with concentration of 5.95 µM, was transferred to a 10.0 mL test tube. The pH of the solution was adjusted by acetate buffer (1M) at 5.0. Then, to perform the extraction process, 0.5 mL of ferrofluid solution was added to the test tube, and the solution was diluted to 10.0 mL with distilled water. The solution was placed in an ultrasonic bath at 30 °C for 30 minutes. FF was separated from the sample solution with a strong magnet (Neodymium magnet). For the elution, 1.0 mL of HCl (1M) was added to the test tube. Finally, the absorption spectra were recorded by UV-vis spectrophotometry at 290 nm.

For preparation of real sample, a 45.0 mL human urine sample was collected as a biological sample from a healthy volunteer in fasting state. Then 10.0 mL of the collected sample was transferred to a centrifuge tube and centrifuged at 5000 rpm for 10 minutes to separate the solutes and sediments. By using centrifugation, broken cells or tissues, solid materials and proteins are precipitated as impurities and a cleaner, lucid and homogeneous solution is obtained. 2.0 mL of the supernatant of the centrifuged sample was diluted with distilled water to a final volume of 50.0 mL in a flask. This solution was stored in the refrigerator for further experiments [37].

3. Results and discussion

3.1. Characterization of CoFe₂O₄ nanoparticles

The FT-IR spectrum of $CoFe_2O_4$ nanoparticles is shown in Fig. 1a. The peak appeared at 583 cm^{-1}, which is related to the stretching vibrations of the Fe-O bond. The peak observed at 420 cm^{-1} confirms the Co-O bond. A sharp peak at 1357 cm^{-1} is devoted to the stretching vibrations of the C-N bond. The observed peaks around 2850 cm^{-1} and 2917 cm^{-1} are

probably due to the CTAB compound and could be attributed to aliphatic stretching C-H bonds. In addition, the peak shown at about 3402 cm^{-1} confirms the presence of a hydroxyl (OH) group of water molecules and the stretching vibrations of this bond. Bending bonds C-H of CTAB were observed in 1835 cm^{-1}, 1911 cm^{-1}, and 1962 cm^{-1} [38].

XRD pattern of synthesized $CoFe_2O_4$ compound is presented in Fig. 1b. The peaks at 18.47°, 30.22°, 35.58°, 43.22°, 53.57°, 57.12°, 62.67° and 74.12° can be assigned to the plates (111), (220), (311), (400), (422), (511), (440) and (533) indexed. As a result, the XRD analysis results show good crystallinity, and no other impurity peaks can be detected [39].

The M-H plot of the synthesized $CoFe_2O_4$ was recorded at room temperature (Fig. 1c). As the magnetic field strength increases, the amount of saturation magnetization (Ms) increases sharply to about 40 emus g^{-1} saturation, indicating that $CoFe_2O_4$ nanoparticles are super-magnetic [40].

To study the thermal stability of $CoFe_2O_4$ nanoparticles, thermogravimetric analysis (TGA) was performed. Due to the high thermal stability, only about 2.4% weight loss of $CoFe_2O_4$ can be detected, when the temperature is up to 700 °C (Fig. 1d).
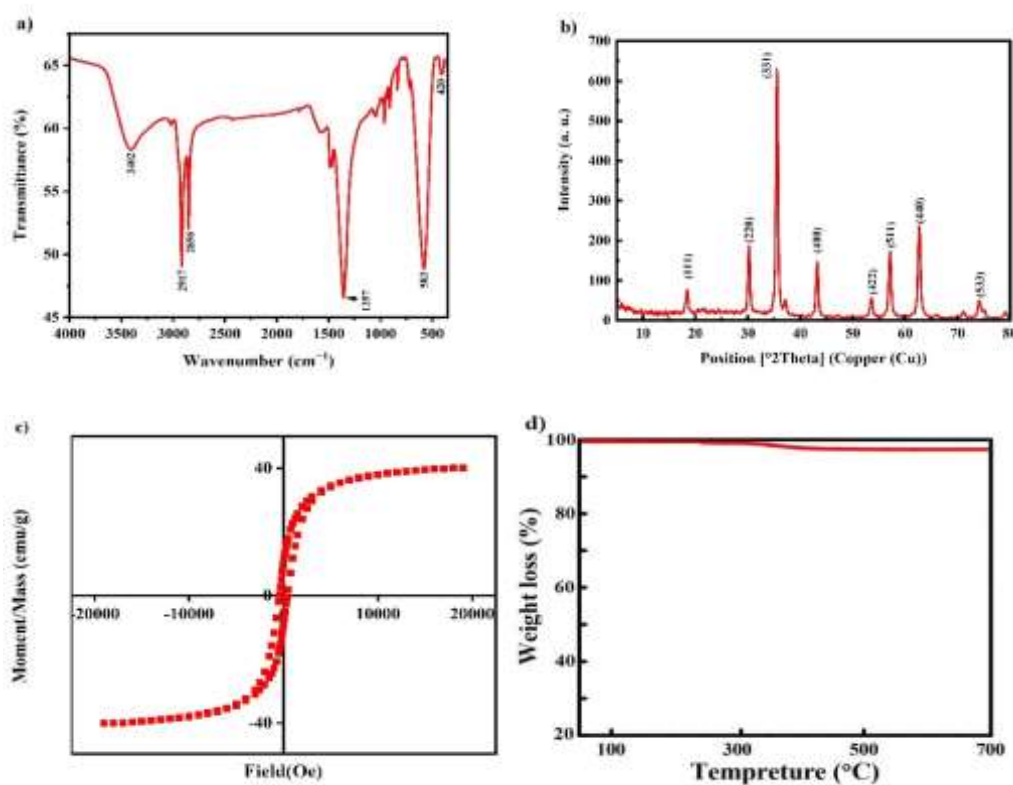

Fig. 1. a) FT-IR spectrum, b) XRD pattern, c) VSM analysis and d) TGA curves of $CoFe_2O_4$ nanoparticles.

The elemental composition of $CoFe_2O_4$ nanoparticles was investigated using X-ray energy diffraction (EDX) spectroscopy (Fig. 2). The EDX analysis for $CoFe_2O_4$ MNPs gave the elemental distribution of Co = 13.97%, Fe = 22.36%, O = 63.67% with the nearly same atomic ratios as in $CoFe_2O_4$ molecule. The results obtained are in good agreement with the reported results in the references, which confirms the accuracy of the synthesis [41].
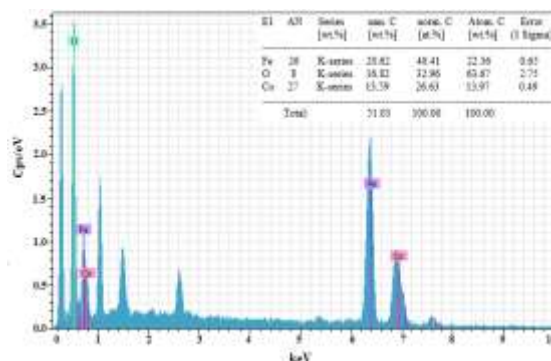
Fig. 2. EDX analysis of $CoFe_2O_4$ nanoparticles.

FE-SEM images of $CoFe_2O_4$ nanoparticles with different magnifications are given in Fig. 3. The spherical structure of cobalt ferrite nanoparticles is seen in the images. The white points on the nanoparticles are probably due to cobalt oxide [42]. The average diameter of $CoFe_2O_4$ nanoparticles was 17.23 nm.
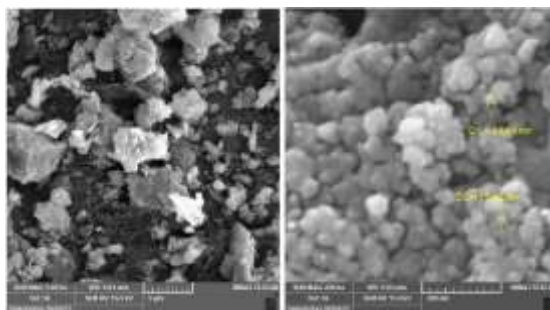

Fig. 3. FE-SEM images of $CoFe_2O_4$ nanoparticles with different magnifications

3.2. Effect of elution conditions

Various eluents such as HNO_3 (1.0 M), HCl (1.0 M), methanol, ethanol, and acetonitrile were chosen and investigated to achieve optimal elution conditions. The maximum response (%ER) was obtained by using HCl 1.0 M (Fig. 4a). The volumes in the range of 0.5- 2.0 mL for HCl (1.0 M) were tested for investigation of eluent volume on the extraction procedure (Fig. 4b). Ultimately, according to the obtained results, the volume of 1.0 mL HCl was selected.
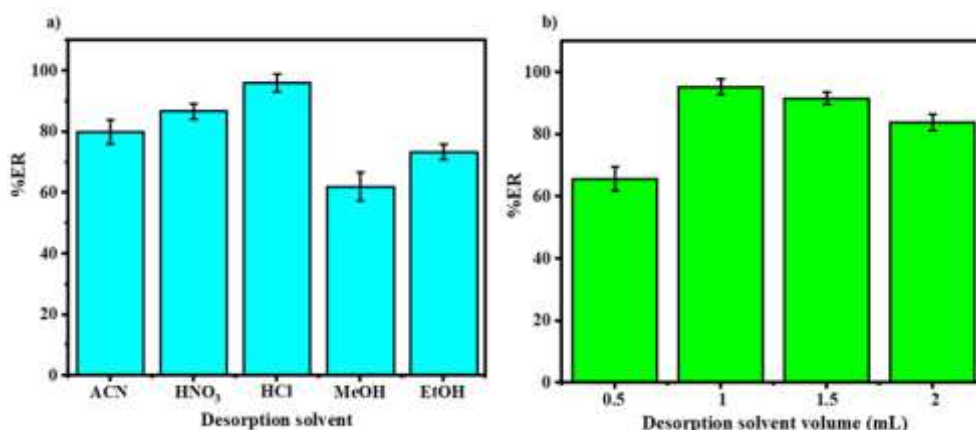

Fig. 4. (a) The effect of desorption solvent type, and (b) The effect of HCl (1.0 M) volume on the determination of UA.

3.3. Experimental Design

In this research, to simultaneously investigate the parameters affecting the process and their interaction effects, multivariate optimization method-based a five-level central composite design (CCD) was used [43]. Four parameters, including pH (A), ferrofluid volume (B), temperature (C) and ultrasonic time (D) were investigated as independent variables. Table 1 shows the variables and their chosen levels based on studies and preliminary experiments. Thirty experiments were designed by CCD and done in three days (3 blocks), and the percentage of uric acid extraction was recorded as the final response.

3.3.1. Analysis of variance (ANOVA)

The significance of the proposed model and the parameters affecting the UA extraction process were evaluated using ANOVA at the 95% confidence level, which is reported in Table 1. The basis of variance analysis is the F test (comparing the ratio of variances with the critical F value). Based on this and considering the p-value (a high F-value and a

.

low p value (p-values < 0.05), the F-value for the model is 92.80, which shows that the selected model is essential and meaningful. Also, if the p-value (probability of error) is less than 0.05, it indicates that an investigated parameter is significant. Therefore, in this research, in addition to the model, the effect of parameters A, B, C, D, CD, A^2 and B^2 is also significant. Another way to evaluate the model is the lack of fit tests. P-value for lack of fit is 0.1875 (> 0.05), which confirms that the model and experimental data are in a good agreement [44]. Correlation between data is checked by R^2 values. The proximity of these values to 1 indicates a good correlation between the data. R^2 obtained from this model was 0.9893. The value of adj-R^2 (0.9787) was obtained, which is close to the value of Pred-R^2 (0.9403) and confirms the validity of the proposed model. Adequate precision (signal-to-noise ratio) greater than 4 indicates adequate discrimination of the model [45]. The adequate precision value obtained from this model was 42.17

Table 1 Independent variables, their levels, and ANOVA results for determination of UA in the CCD.

Variable	Symbol	Levels of variable				
		$-\alpha$	-1	0	$+1$	$+\alpha$
pH	A	4	5	6	7	8
Vol. FF (mL)	B	0.2	0.3	0.4	0.5	0.6
Temp (°C)	C	25	30	35	40	45
Ult. time (min)	D	15	20	25	30	35

Source	Sum of Squares	DF[a]	Mean Square	F Value	p-value Prob > F	
Model	13829.85	14	987.85	92.80	< 0.0001	significant
A	6499.99	1	6499.99	610.62	< 0.0001	significant
B	145.41	1	145.41	13.66	0.0024	significant
C	1723.52	1	1723.52	161.91	< 0.0001	significant
D	154.02	1	154.02	14.47	0.0019	significant
AB	0.29	1	0.29	0.027	0.8718	
AC	1.10	1	1.10	0.10	0.7529	
AD	38.52	1	38.52	3.62	0.0779	
BC	25.83	1	25.83	2.43	0.1416	
BD	2.47	1	2.47	0.23	0.6373	
CD	75.90	1	75.90	7.13	0.0183	significant
A^2	243.34	1	243.34	22.86	0/0003	significant
B^2	4409.57	1	4409.57	414.24	< 0.0001	significant
C^2	0.50	1	0.50	0.047	0.8315	
D^2	3.76	1	3.76	0.35	0.5616	
Residual	149.03	14	10.64			
Lack of Fit	108.72	10	10.87	1.08	0.5139	not significant
Pure Error	40.31	4	10.08			
Cor Total[b]	13992.75	29				

[a] Degrees of freedom.

[b] Totals of all information corrected for the mean.

3.3.2. Interpretation of the simultaneous effect of main parameters and diagnostic plots

In order to examine the simultaneous effect of the main parameters on the % ER of UA, 3-D response surface and contour plots were used (Fig. 5a–c). Fig. 5a shows the simultaneous effect of pH and ferrofluid volume (extraction phase) on the process of UA extraction. Maximum response (%ER$_{UA}$) was observed in the high amounts of ferrofluid volume (> 0.45 mL). In volumes lower than 0.45 mL, sufficient contact surface is not provided to the target analyte, therefore effective interactions and thus the mass transfer of the analyte to the extraction phase is reduced. Also, it becomes difficult to collect the extraction phase. At pH less than 6.0, due to the protection of UA from degradation, the tendency of the UA to dissociate decreases. So the pH range of 5.0 to 5.5 is suitable for extracting UA. Temperature affects the solubility of organic solvent in water, distribution coefficient and mass transfer of target analytes. As shown in Fig. 5b, increasing the temperature of the solution up to 32°C increases the diffusion and mass transfer kinetics of UA to the organic phase and thus increases the extraction efficiency. However, at temperatures higher than 32°C, the extraction efficiency will probably decrease due to the instability and degradation of UA. Therefore, the temperature range of 30°C to 32°C as the optimal temperature range has the most effect on the extraction process. The simultaneous effect of ferrofluid volume and ultrasonic time on the percentage of UA extraction is shown in Fig. 5c.

Maximum response was obtained at ultrasonic times of more than 26 minutes. Because the ferrofluid is sufficiently dispersed in the solution using .

ultrasonic waves, and thus a large contact surface is available to trap the analytes
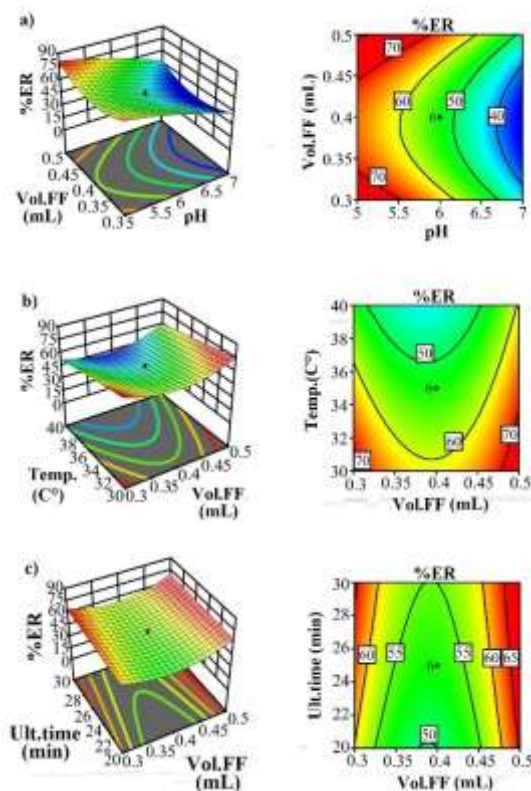

Fig. 5. 3-D response surface and counter plots for determination of UA. (a) pH and volume of ferrofluid, (b) Volume of ferrofluid and temperature, and (c) Volume of ferrofluid and ultrasonic time.

The normal probability plot (NPP) examines the normal distribution of the residuals. If the distribution of the residuals is normal, the resulting diagram will be a straight line. According to NPP obtained in the proposed UA extraction method, the distribution of residues is normal and around a straight line (Fig. 6a). This normal distribution shows that the errors created during the process were completely random and the proposed model has no

systematic error. A plot of predicted values versus the actual values examines the difference between the adjusted correlation coefficient (adj-R^2) and the model correlation coefficient (R^2), so the data should be centered on a straight line. According to Fig. 6b in this study, the predicted and actual values have a good correlation. Therefore, based on the results and evidence presented in the graph, the adequacy and validity of the presented model are proved.
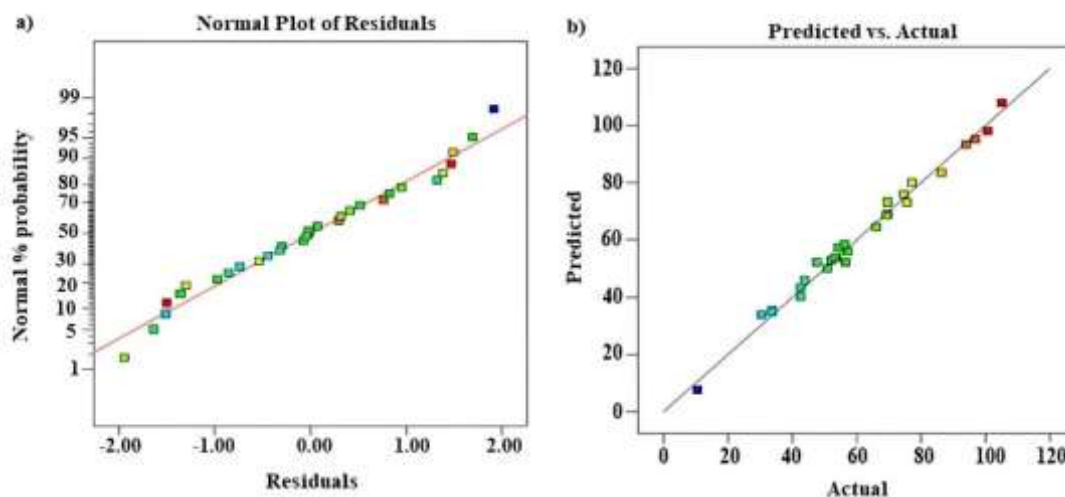
Fig. 6. Diagnostic plots for determination of UA. a) Normal probability plot, and b) The predicted values vs. the actual values.

3.3.3. Optimal points for LPME-FF method

The optimal condition of the introduced method was determined using the desirability function, which is a common and efficient method and includes values between zero and one. The closer the value of this function is to one, the more confidently it can be said that the predicted values are the optimal points in the process [46]. Based on the prediction of Design-Expert® software and with the desirability value of 0.938, the optimal points in the process of UA extraction were pH = 5.0, ferrofluid volume = 0.5 mL, temperature = 30 °C and, ultrasonic time = 30 min. After four replicates in optimal conditions, the %ER of UA was 93.35±2.4, which was close to the response predicted by the software (92.63±1.7).

3.4. Ionic strength

In general, the addition of salt, called the salting-out effect, reduces the solubility of the analyte in the aqueous phase, increases the mass transfer of the analyte to the organic phase, and thus increases the extraction efficiency [47]. Accordingly, the effects of different concentrations of NaCl (0–1.0 M) were investigated. The results showed that the addition of salt does not have a significant effect on %ER of UA. Therefore, subsequent experiments were performed in the absence of salt.

3.5. Selectivity study

The potential interference of several different chemical species (common cations and anions and some organic compounds) that exist together with UA in real samples and may affect the selectivity of the proposed method was investigated. If the studied species causes more than 5% error in the response signal, it is interference compound. The sample solutions containing UA (5.95 μM) and the studied species (different amounts) were analyzed using the proposed method. Based on the experimental results reported in Table 2, common ions (cations and anions), even with very high ratios, do not affect the %ER of UA, but Cu^{2+} and Fe^{2+} ions in ratios >50 cause interference. Sugars (glucose, sucrose and, lactose) and cysteine as an amino acid do not affect the measured signal to an acceptable extent. Folic acid until ratio 30, dopamine and glutamic acid up ratio 20 do not interfere. Ascorbic acid and urea can be tolerated up to 3–fold. These results confirm the selectivity of the LPME-FF-UV-Vis method in the studied linear range and therefore the recommended method is suitable for the analysis of UA in real sample.

Table 2 The effect of different substances on the extraction recovery of UA (5.95 μM).

Foreign substances	Tolerance ratio (μM/μM)
Ca^{2+}, Ni^{2+}, K^+, PO_4^{3-}, SO_4^{2-}, NO_3^-, Cl^-	4500 (3.1)[a]
Mg^{2+}, Zn^{2+}, Co^{2+}, Na^+	1800 (2.9)
Glucose, Sucrose & Lactose	700 (2.4)
Cysteine	80 (3.6)
Cu^{2+}, Fe^{2+}	50 (3.1)
Folic acid	30 (4.3)
Dopamine, Glutamic acid	20 (3.8)
Ascorbic acid, Urea	3 (4.0)

a. The relative standard deviation (n=3).

3.6. Analytical features

After optimization, the analytical features of the developed method were evaluated. The calibration plot of the UA showed a linear range between 0.42 and 238 μM, with a correlation coefficient higher than 0.99. The limit of detection (LOD) and quantification (LOQ) were found to be 0.12 μM and 0.39 μM, respectively. Also, the methods precision was evaluated through the study of inter-day and intra-day precisions (as RSD %). The RSD (%) values for the intra-day and inter-day precisions were 2.1 and 3.0 %, respectively. UV-Vis absorption spectra of UA in different concentrations are given in Fig. 7.
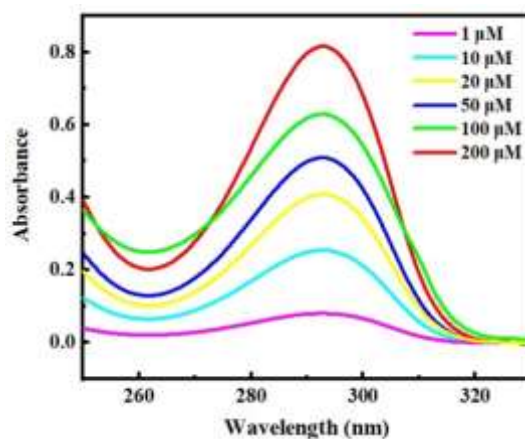

Fig. 7. UV-Vis absorption spectra of UA in different concentrations.

3.7. Adsorption mechanism of uric acid

The efficiency of the extraction process depends significantly on the binding energies established between supramolecular solvent (Ss) and the analytes (ionic > hydrogen bonding > dipole-dipole, etc.). Owing to the amphiphilic nature of the molecules, the resulting complexes have regions with different polarities that create diverse interactions with analytes [48,49]. Ferrofluid used in this research composed of inverted aggregates of 1-decanol as an Ss that spontaneously form in THF: water solution provided an effective environment for separation and preconcentration of UA. Ss made of alkanols provide mixed-mode solvation properties for medium polar and nonpolar analytes by hydrogen bonding and dispersion interactions. Since 1-decanol has a medium length hydrocarbon chain, both hydrogen bonding and dispersion interactions are expected to be the main extraction forces [50]. The structure and nature of the

Table 3 Determination of UA in biological sample of human urine with the proposed method (n=3).

Matrix	LDR (μM)	LOD (μM)	LOQ (μM)	R^2	Spiked (μM)	Found (μM)	Recovery (%)	HPLC-UV (μM)
Human urine	0.59-178.50	0.18	0.59	0.985	0	14.22 ± 1.02^a	-	12.84 ± 1.35
					2.97	16.03 ± 1.09	94	15.62 ± 1.40
					5.95	18.18 ± 0.99	103	17.47 ± 1.52

[a] The standard deviation.

functional groups in the UA molecule show the potential of different types of interactions. UA contains hydrogen donor and acceptor atoms. Therefore, 1-decanol reverse micelle solubilizes UA mainly due to the mixed-state mechanism and the availability of multiple binding sites on hydrophobic

3.8. Applications

To assess the feasibility and accuracy, the introduced method was investigated for pre-concentration and determination of UA in the biological sample of human urine. Based on this, certain concentrations of target analyte were added to the samples, and after preconcentration and extraction in optimal conditions, a calibration curve was drawn. The relative recovery percentage (%RR) was also calculated from equation (1), where C_{found}, C_{real}, and C_{add} are the concentration obtained after analyte spiking, the concentration of UA in the real sample before spiking (blank solution) and the added concentration of UA to the real sample.

$$\%RR = ((C_{found} - C_{real})/C_{add}) * 100 \qquad (1)$$

The results are reported in Table 3. The %RR between 94 % and 103 % confirms the applicability and high accuracy of the proposed method. LPME-FF coupled with the spectrophotometry method provided statistical results very close to HPLC-UV as the reference method, which indicates the validity performance of the proposed approach.

3.9. Comparison with pervious work

To illustrate the performance of the recommended method, a comparison study with pervious works was carried out (Table 4). Accordingly, regarding LOD, the proposed method was superior to all methods. The RSD% of the introduced method was comparable to or better than most methods. It can be

interactions in the hydrocarbon tail and hydrogen bonds of polar alcohol groups with UA. These interactions are essential for both increasing performances of desired analyte extraction and decreasing the extraction time.

said that the working range was compatible with all methods. Also, the extraction recovery percentages is satisfactory. These criteria certify the superior ability of the LPME-FF-UV-Vis detection procedure in trace UA determination in complex matrices.

4. Conclusion

In this study, an LPME-FF method combined with UV-Vis was presented for preconcentration, separation, and determination of UA in human urine samples. The magnetic cobalt ferrite nanoparticles ($CoFe_2O_4$) were used together with a supramolecular solvent consisting of THF and 1-decanol to prepare ferrofluid. The ferrofluid was convenient for the use of low-density extraction solvents such as Ss without any special device and complicated operation. The presented microextraction method lacks tedious steps of conventional microextraction methods, such as centrifugation, refrigeration and thawing of organic solvents. The central composite design was used to significantly reduce the number of experiments, save time and material consumption, and to examine the effective parameters on the UA extraction process simultaneously. Validity of the proposed method resulted in appropriate analytical figures of merit such a wide linear range (0.42–238 μM), low LOD (0.12 μM), good repeatability (2.1%) and reproducibility (3.0 %). The matrix influences with

the developed procedure were reasonably tolerable. Eventually, the application of the LPME-FF-UV-Vis method to human urine sample with the relative recovery percentages above of 94 % proved the practicality and reliability of the proposed method. The validity of the proposed method was confirmed by the HPLC-UV as the reference method. Thus, the introduced LPME-FF technique offers outstanding advantages such as simplicity of the extraction, good repeatability and reproducibility, and environmental friendliness.

Table 4 Comparison of the proposed method with reported methods in the determination of UA.

Method	Matrix	LDR (μM)	LOD (μM)	LOQ (μM)	RSD%	Recovery (%)	Ref
Fluorescence	Serum	0.5-30	0.14	0.46	-	95-104	51
Voltammetric	Clinical Serum	5-100	0.19	0.63	0.9	93-107	52
Voltammetric	Human urine	5-50	0.12	0.39	4.7	92-107	53
Electrochemistry	Urine	5-200	0.17	0.56	2.46-3.01	99.7-101.7	54
Electrochemistry	Human urine	10-100	3.75	12.37	-	91.3-113.4	55
Colorimetric – UV	Blood serum	1-120	0.25	0.8	2.4	-	56
Ratiometric – FL	Cow Serum	0.7-60	0.21	0.69	≤ 4.6	102.5–103.3	57
LPME-FF-UV-Vis	Human urine	0.42-238	0.12	0.39	2.1	94-103	This work

References

[1] Waryani, B., Tahira, A., Ameen, S., Willande, M., Abbasi, A. R., & Ibupoto, Z. H. (2020). The Enzyme Free Uric Acid Sensor Based on Iron Doped CuO Nanostructures for the Determination of Uric Acid from Commercial Seafood. *Journal of Electronic Materials*, 49(10), 6123-9.

[2] Zheng, W., Zhao, M., Liu, W., Yu, S., Niu, L., Li, G., & Liu, W. (2018). Electrochemical sensor based on molecularly imprinted polymer/reduced graphene oxide composite for simultaneous determination of uric acid and tyrosine. *Journal of Electroanalytical Chemistry*, 813, 75-82.

[3] Mizuguchi, H., Fujiki, S., Shibata, T., Oishi, M., Iiyama, M., Takayanagi, T., & Yeh, M.-H. (2023). A flow-based enzyme-free biosensor fabricated using track-etched membrane electrodes: Selective and sensitive detection of uric acid. *Sensors and Actuators B: Chemical*, 383, 133588.

[4] Chang, Y.-J., Lee, M.-C., & Chien, Y.-C. (2022). Quantitative determination of uric acid using paper-based biosensor modified with graphene oxide and 5-amino-1,3,4-thiadiazole-2-thiol. *SLAS Technology*, 27, 54-62.

[5] Wu, C., Zhu, L., Lu, Q., Li, H., Zhang, Y., & Yao, S. (2019). A dual-signal colorimetric and ratiometric fluorescent nanoprobe for enzymatic determination of uric acid by using silicon nanoparticles. *Microchimica Acta*, 186(12), 754.

[6] Ratautaite, V., Samukaite-Bubniene, U., Plausinaitis, D., Boguzaite, R., Balciunas, D., Ramanaviciene, A., & Ramanavicius, A. (2021). Molecular Imprinting Technology for Determination of Uric Acid. *International Journal of Molecular Sciences*, 22(9), 5032.

[7] Mishima, E., Anzai, N., Miyazaki, M., & Abe, T. (2020). Uric acid elevation by favipiravir, an antiviral drug. *The Tohoku Journal of Experimental Medicine*, 251(2), 87-90.

[8] Zhao, H., Wang, Z., Jiao, X., Zhang, L., & Lv, Y. (2012). Uricase-based highly sensitive and selective spectrophotometric determination of uric acid using BSA-stabilized Au

nanoclusters as artificial enzyme. *Spectroscopy Letters*, 45(7), 511-9.

[9] Bian, W., Wang, L., Zhang, N., & Jiang, C. (2014). Spectrofluorimetric method for the determination of uric acid in human serum. *Journal of Analytical Chemistry*, 69, 480-4.

[10] Thanh, T. S., Qui, P. T., Tu, N. T. T., Toan, T. T. T., Hoa, T. T. B., Son, L. V. T., & Khieu, D. Q. (2021). Electrochemical determination of uric acid in urine by using zeolite imidazolate framework-11 modified electrode. *Journal of Nanomaterials*, 2021.

[11] Kong, M., Wei, W., Wang, W., Chen, H., & He, J. (2021). A novel metal organic gel with superior oxidase-like activity for efficient and sensitive chemiluminescence detection of uric acid. *Spectrochimica Acta Part A: Molecular and Biomolecular Spectroscopy*, 257, 119773.

[12] Raj V., & Alex S. (2022). Phosphotungstic Acid Capped Gold Nanoparticles for Spectrophotometric Determination of Uric Acid in Diagnostics of Gout. *Journal of Analytical Chemistry*, 77(10), 1267-73.

[13] Chen, Y., Ji, P., Ma, G., Song, Z., Tang, B. Q., & Li, T. (2021). Simultaneous determination of cellular adenosine nucleotides, malondialdehyde, and uric acid using HPLC. *Biomedical Chromatography*, 35(10), e5156.

[14] Fathi, M., Rajabi, H. R., Khajehsharifi, H., & Gorjizadeh Kohvadeh, A. (2024). Application of liquid-liquid microextraction based on deep eutectic solvent for preconcentration and spectrophotometric determination of purpurin. *Applied Chemistry Today*, 19(70), 135-150.

[15] Tsanaktsidou, E., Markopoulou, C. K., Tzanavaras, P. D., & Zacharis, C. K. (2022). Homogeneous liquid phase microextraction using hydrophilic media for the determination of fluoroquinolones in human urine using HPLC-FLD. *Microchemical Journal*, 172, 106906.

[16] Mohammadi, S.Z.; Rohani, T.; & Bahadori, L. (2017) Magnetic solid-phase extraction based on modified iron oxide nanoparticles for the preconcentration of ultra-trace amounts of copper ions in the environmental and plant samples and its determination using FAAS. *Communications in Soil Science and Plant Analysis,* 48: 1359–1368.

[17] Sun, X., Wang, J., Li, Y., Jin, J., Yang, J., Li, F., & Chen, J. (2014). Highly class-selective solid-phase extraction of bisphenols in milk, sediment and human urine samples using well-designed dummy molecularly imprinted polymers. *Journal of Chromatography A*, 1360, 9–16.

[18] Panhwar, A. H., Tuzen, M., & Kazi, T. G. (2018). Deep eutectic solvent based advance microextraction method for determination of aluminum in water and food samples: Multivariate study. *Talanta*, 178, 588-593.

[19] Yang, D., Li, G., Wu, L., & Yang, Y. (2018). Ferrofluid-based liquid-phase microextraction: analysis of four phenolic compounds in milks and fruit juices. *Food chemistry,* 261, 96-102.

[20] Kokosa JM. (2021). A guide to recent trends in green applications of liquid phase microextraction for bioanalytical sample

preparations. *Sustainable Chemistry and Pharmacy*, 22, 100478.

[21] Mirzajani, R., & Karami, S. (2021). Dispersive micro solid phase extraction based on surface magnetic molecular imprinted polymer and deep eutectic solvent with optimization by central composite design for determination of dipyridamole in pharmaceutical and biological samples. *Applied Chemistry Today*, 16(58), 47-62.

[22] Rostamzadeh, B., Ebrahimi, N., & Sadeghi, R. (2024). Study on the salting effect of choline chloride on aqueous solutions of imidazolium-based ionic liquids via the isopiestic measurements. *Applied Chemistry Today*, 19(70), 29-44.

[23] Sajid M, Kalinowska K., & Płotka-Wasylka J. (2021). Ferrofluids based analytical extractions and evaluation of their greenness. *Journal of Molecular Liquids,* 339, 116901.

[24] Moradi M, Yamini Y., & Feizi N. (2021). Development and challenges of supramolecular solvents in liquid-based microextraction methods. *TrAC Trends in Analytical Chemistry*, 138, 116231.

[25] Socoliuc, V., Avdeev, M., Kuncser, V., Turcu, R., Tombácz, E., & Vekas, L. (2022). Ferrofluids and bio-ferrofluids: looking back and stepping forward. *Nanoscale*, 14(13), 4786-886.

[26] Amirabadizadeh, A., Salighe, Z., Sarhaddi, R., & Lotfollahi, Z. (2017). Synthesis of ferrofluids based on cobalt ferrite nanoparticles: Influence of reaction time on structural, morphological and magnetic properties. *Journal of Magnetism and Magnetic Materials,* 434, 78-85.

[27] Gingasu, D., Mindru, I., Patron, L., Calderon-Moreno, J. M., Mocioiu, O. C., Preda, S., & Chifiriuc, M. C. (2016). Green synthesis methods of $CoFe_2O_4$ and $Ag-CoFe_2O_4$ nanoparticles using hibiscus extracts and their antimicrobial potential. *Journal of Nanomaterials,* 2016, 2106756.

[28] Zohrabi, P., Shamsipur, M., Hashemi, M., & Hashemi, B. (2016). Liquid-phase microextraction of organophosphorus pesticides using supramolecular solvent as a carrier for ferrofluid. *Talanta*, 160, 340-6.

[29] Caballo, C., Sicilia, M. D., & Rubio, S. (2017). Chapter 5 - Supramolecular Solvents for Green Chemistry. In F. Pena-Pereira & M. Tobiszewski (Eds.), *The Application of Green Solvents in Separation Processes* (pp. 111-137).

[30] Firouzabadi, Z. D., Shabani, A. M. H., Dadfarnia, S., & Ehrampoush, M. H. (2017). Preconcentration and speciation of thallium by ferrofluid based dispersive solid phase extraction and flame atomic absorption spectrometry. *Microchemical Journal*, 130, 428-35.

[31] Fasih Ramandi N., & Shemirani F. (2015). Surfacted ferrofluid based dispersive solid phase extraction; a novel approach to preconcentration of cationic dye in shrimp and water samples. *Food Chemistry*, 185, 398-404.

[32] Wang, H., Yan, H., Wang, C., Chen, F., Ma, M., Wang, W., & Wang, X. (2012). Analysis of phenolic pollutants in human samples by high performance capillary electrophoresis based on pretreatment of

ultrasound-assisted emulsification microextraction and solidification of floating organic droplet. *Journal of Chromatography A*, 1253, 16-21.

[33] Heydari, R., & Zarabi, S. (2014). Development of combined salt-and air-assisted liquid–liquid microextraction as a novel sample preparation technique. *Analytical Methods*, 6(21), 8469-8475.

[34] Shamsipur, M., & Hashemi, B. (2015). Extraction and determination of polycyclic aromatic hydrocarbons in water samples using stir bar sorptive extraction (SBSE) combined with dispersive liquid–liquid microextraction based on the solidification of floating organic drop (DLLME-SFO) followed by HPLC-UV. *RSC advances,* 5(26), 20339-20345.

[35] Yang D, Li G, Wu L., & Yang Y. (2018). Ferrofluid-based liquid-phase microextraction: Analysis of four phenolic compounds in milks and fruit juices. *Food Chemistry*, 261, 96-102.

[36] Ehsan, M. F., Fazal, A., Hamid, S., Arfan, M., Khan, I., Usman, M., & Ashiq, M. N. (2020). $CoFe_2O_4$ decorated $g\text{-}C_3N_4$ nanosheets: New insights into superoxide anion mediated photomineralization of methylene blue. *Journal of Environmental Chemical Engineering, 8(6), 104556.*

[37] Zuo, Y., Yang, Y., Zhu, Z., He, W., & Aydin, Z. (2011). Determination of uric acid and creatinine in human urine using hydrophilic interaction chromatography. *Talanta*, 83(5), 1707-1710.

[38] Joseph, A., Thangaraj, B., Gomathi, R., & Arockia Raj, A. (2017). Synthesis and characterization of cobalt ferrite magnetic nanoparticles coated with polyethylene glycol. 71-77.

[39] Chang, S., Zhang, Q., Lu, Y., Wu, S., & Wang, W. (2020). High-efficiency and selective adsorption of organic pollutants by magnetic $CoFe_2O_4$/graphene oxide adsorbents: Experimental and molecular dynamics simulation study. *Separation and Purification Technology, 238, 116400.*

[40] Mushtaq, M., Imran, M., Bashir, S., Kanwal, F., & Mitu, L. (2016). Synthesis, structural and biological studies of cobalt ferrite nanoparticles. *Bulgarian Chemical Communications, 48(3), 565-570.*

[41] Kombaiah, K., Vijaya, J. J., Kennedy, L. J., Bououdina, M., Ramalingam, R. J., & Al-Lohedan, H. A. (2017). Comparative investigation on the structural, morphological, optical, and magnetic properties of $CoFe_2O_4$ nanoparticles. *Ceramics International, 43(10), 7682-7689.*

[42] Sapna, Budhiraja, N., Kumar, V., & Singh, S. K. (2018). Synergistic effect in structural and supercapacitor performance of well dispersed $CoFe_2O_4$/Co_3O_4 nano-hetrostructures. *Ceramics International, 44(12), 13806-13814.*

[43] Dadras Moghaddam H, Khani R., & Khodaei B. (2022). Liquid-phase microextraction of ascorbic acid in food and pharmaceutical samples using ferrofluid-based on cobalt ferrite ($CoFe_2O_4$) nanoparticles. *Microchemical Journal*, 183, 108006.

[44] Jalalifar, A., Zare-Shahabadi, V., & Sayyahi, S. (2020). Synthesis and application of Fe3O4/PANIL nanocomposite as efficient adsorbent in the removal of styrene from waste

water: Optimizing and modelling the process. *Applied Chemistry Today*, 15(54), 137-152.

[45] Nikseresht, A., & Normohamadi, H. (2024). Development and Optimization Synthesis of MIL-101 (Cr) by Ultrasound Irradiation Using Response Surface Methodology. *Applied Chemistry Today*, 19(71), 223-246.

[46] Khani R, Ghalibafan M., & Farrokhi A. (2020). Performance of metal-organic framework as an excellent sorbent for highly efficient and sensitive trace determination of anthracene in water and food samples. *Environmental Science and Pollution Research*, 27(21), 26305-14.

[47] Yang, D., Li, X., Meng, D., & Yang, Y. (2018). Carbon quantum dots-modified ferrofluid for dispersive solid-phase extraction of phenolic compounds in water and milk samples. *Journal of Molecular Liquids*, 261, 155-61.

[48] Avval, M. M., & Khani, R. (2022). Eco-friendly and affordable trace quantification of riboflavin in biological and food samples using a supramolecular solvent based liquid–liquid microextraction. *Journal of Molecular Liquids*, *362*, 119725.

[49] Peyrovi, M., & Hadjmohammadi, M. (2015). Extraction optimization of Loratadine by supramolecular solvent-based microextraction and its determination using HPLC. *Journal of Chromatography B*, 980, 41-47.

[50] Ballesteros-Gómez, A., & Rubio, S. (2012). Environment-responsive alkanol-based supramolecular solvents: characterization and potential as restricted access property and mixed-mode extractants. *Analytical chemistry*, 84(1), 342-349.

[51] Cao, D., Luo, Y.-X., Liu, W.-P., Li, Y.-S., & Gao, X.-F. (2021). Enzyme-free fluorescence determination of uric acid and trace Hg (II) in serum using Si/N doped carbon dots. *Spectrochimica Acta Part A: Molecular and Biomolecular Spectroscopy*, 263,120182.

[52] Metto, M., Eramias, S., Gelagay, B., & Washe, A. P. (2019). Voltammetric Determination of Uric Acid in Clinical Serum Samples Using DMF Modified Screen Printed Carbon Electrodes. *International Journal of Electrochemistry,* 2019, 6318515.

[53] Feng, S., Yu, L., Yan, M., Ye, J., Huang, J., & Yang, X. (2021). Holey nitrogen-doped graphene aerogel for simultaneously electrochemical determination of ascorbic acid, dopamine and uric acid, *Talanta*, 224, 121851.

[54] Ahammad, A. S., Odhikari, N., Shah, S. S., Hasan, M. M., Islam, T., Pal, P. R., & Aziz, M. A. (2019). Porous tal palm carbon nanosheets: preparation, characterization and application for the simultaneous determination of dopamine and uric acid. *Nanoscale Advances*, 1(2), 613-26.

[55] Wang, Y., Liu, X., Lu, Z., Liu, T., Zhao, L., Ding, F., & Rao, H. (2019). Molecularly imprinted polydopamine modified with nickel nanoparticles wrapped with carbon: fabrication, characterization and electrochemical detection of uric acid. *Microchimica Acta*, 186(7), 414.

[56] Pan, Y., Yang, Y., Pang, Y., Shi, Y., Long, Y., & Zheng, H. (2018). Enhancing the peroxidase-like activity of ficin via heme

binding and colorimetric detection for uric acid, *Talanta*, 185, 433-8.

[57] Pang S. (2019). A ratiometric fluorescent probe for detection of uric acid based on the gold nanoclusters-quantum dots nanohybrid. *Spectrochimica Acta Part A: Molecular and Biomolecular Spectroscopy*, 222, 117233.